Development 139, 423-436 (2012) doi:10.1242/dev.075499

Clonal and molecular analysis of the prospective anterior neural boundary in the mouse embryo

Marieke Cajal[1], Kirstie A. Lawson[2,*], Bill Hill[2], Anne Moreau[1], Jianguo Rao[2], Allyson Ross[2], Jérôme Collignon[1] and Anne Camus[1,*]

SUMMARY

In the mouse embryo the anterior ectoderm undergoes extensive growth and morphogenesis to form the forebrain and cephalic non-neural ectoderm. We traced descendants of single ectoderm cells to study cell fate choice and cell behaviour at late gastrulation. In addition, we provide a comprehensive spatiotemporal atlas of anterior gene expression at stages crucial for anterior ectoderm regionalisation and neural plate formation. Our results show that, at late gastrulation stage, expression patterns of anterior ectoderm genes overlap significantly and correlate with areas of distinct prospective fates but do not define lineages. The fate map delineates a rostral limit to forebrain contribution. However, no early subdivision of the presumptive forebrain territory can be detected. Lineage analysis at single-cell resolution revealed that precursors of the anterior neural ridge (ANR), a signalling centre involved in forebrain development and patterning, are clonally related to neural ectoderm. The prospective ANR and the forebrain neuroectoderm arise from cells scattered within the same broad area of anterior ectoderm. This study establishes that although the segregation between non-neural and neural precursors in the anterior midline ectoderm is not complete at late gastrulation stage, this tissue already harbours elements of regionalisation that prefigure the later organisation of the head.

KEY WORDS: Mouse embryo, Fate map, Neural plate, Anterior neural ridge, Transcription factors, 3D reconstruction

INTRODUCTION

During gastrulation, pluripotent epiblast cells that do not ingress through the primitive streak (PS) go on to form the neuroectoderm, the surface ectoderm and the amnion ectoderm (Snow, 1977; Tam, 1989; Lawson et al., 1991; Quinlan et al., 1995). The anterior neuroectoderm is a uniform sheet of neuroepithelial cells that gives rise to the forebrain: by the end of somitogenesis, this complex structure comprises the telencephalon and the eyes dorsally and ventrally, the hypothalamus and the diencephalon.

In the mouse, embryological and molecular evidence indicates that, from embryonic day (E) 7.0, signals from the anterior mesendoderm initiate ectoderm regionalisation, well before molecular and morphological signs of neural plate formation are detected (Ang and Rossant, 1993; Ang et al., 1994; Pevny et al., 1998; Wood and Episkopou, 1999; Pfister et al., 2007). *Otx2*, *Six3* and *Hesx1*, which encode transcription factors essential to forebrain development, are expressed in specific domains within the anterior ectoderm of the gastrulating embryo (Rhinn et al., 1999; Martinez-Barbera et al., 2000; Martinez-Barbera et al., 2001; Simeone and Acampora, 2001; Lagutin et al., 2003). At the beginning of neurulation (E8.5), further regionalisation of the anterior neural plate involves cell-specific responses to extrinsic signals produced by axial midline tissues and non-neural ectoderm (Rubenstein and Shimamura, 1998; Wilson and Houart, 2004). FGF signalling in the anterior neural ridge (ANR), at the junction between anterior neural and non-neural ectoderm, regulates forebrain development and patterning (Shimamura and Rubenstein, 1997; Shanmugalingam et al., 2000; Paek et al., 2009). Various anterior defects, including absence or reduction of the telencephalic vesicles, eyes, olfactory placodes and frontonasal structures, and truncation of the structures rostral to the zona limitans intrathalamica (ZLI), have been consistently associated with a reduction of *Fgf8* expression in the ANR (Dattani et al., 1998; Meyers et al., 1998; Acampora et al., 2000; Crossley et al., 2001; Kobayashi et al., 2002; Suda et al., 2001; Tian et al., 2002; Zoltewicz et al., 2009; Vieira et al., 2010).

Genetic studies and earlier investigations of cell fate in the anterior ectoderm, relying on orthotopic grafts (Beddington, 1981; Tam, 1989), provided important insights into the early steps of forebrain development. Yet, we still have a limited understanding of how anterior ectoderm develops into neural and non-neural derivatives and, in particular, how the ANR signalling centre forms (Eagleson et al., 1995; Houart et al., 1998). Lineage analysis of single cells (Lawson et al., 1991) is required to define whether, at late gastrulation stage, the anterior ectoderm is composed of distinct region-specific progenitors, a mixed population of progenitors with distinct fates, or a single multipotent cell population. Single-cell resolution is also needed to understand whether the ANR is a separate lineage or whether it arises in response to spatial cues as the neural plate matures. Finally, clonal analysis is essential to investigate whether a given gene marks a prospective tissue and functions as a putative lineage determinant.

We traced the descendants of single cells to describe the transformation of late gastrulation stage anterior midline ectoderm into the surface ectoderm and forebrain at early somite stages. Evidence for segregation of neural and non-neural progenitors and significant regionalisation of prospective fate was found. Importantly, our results delineate a rostral limit to forebrain contribution at a position that is significantly more distal than previously described. We provide a comprehensive spatiotemporal

[1]Université Paris Diderot, Sorbonne Paris Cité, Institut Jacques Monod, UMR7592 CNRS, F-75013 Paris, France. [2]MRC Human Genetics Unit at the MRC Institute of Genetics and Molecular Medicine at the University of Edinburgh, Western General Hospital, Edinburgh EH4 2XU, UK.

*Authors for correspondence (kirstie.lawson@hgu.mrc.ac.uk; camus.anne@ijm.univ-paris-diderot.fr)

Accepted 7 November 2011

atlas of anterior gene expression at stages crucial for anterior ectoderm regionalisation and neural plate formation. Its comparison with the fate map showed that several transcription factors are restricted to subdomains that correlate with regions of prospective fate, but that these factors do not define a specific lineage. A 3D representation of clone spatial distribution at the early somite stage showed that the anterior neural border is not fully defined at late gastrulation stage, nor are early regional subdivisions of the presumptive forebrain territory established. In addition, our results show that ANR progenitors are dispersed over a broad area of the anterior ectoderm where neural precursors reside. ANR and forebrain descendants often share a common progenitor.

MATERIALS AND METHODS

Embryos

Mouse embryos were obtained from [C57BL/6J × CBA] F1 matings. The stage at injection ranged from late streak (LS) to late streak/early bud (LSEB). At the LS stage, the anterior end of the streak has reached the distal tip and the amniochorionic fold is nearly complete. At the LSEB stage, the node starts to be obvious, the amniochorionic fold component parts have just fused and the allantoic bud is just visible. Experiments were performed in accordance with European and French Agricultural Ministry guidelines for the care and use of laboratory animals (Council directives 2889 and 86/609/EEC).

Embryo culture and single-cell labelling

The procedures for embryo culture, iontophoretic injection into single cells and labelled cell identification were as previously described (Beddington and Lawson, 1990; Lawson et al., 1991; Perea-Gomez et al., 2001) with the following modifications. Impaled ectoderm cells showing a stable drop in potential of 10 mV or more were injected with a mixture of 8.7% horseradish peroxidase (HRP; ~1000 U/mg, Boehringer/Roche) and 1.3% lysinated tetramethylrhodamine dextran (LRDX; 10^3 M_r, Molecular Probes) in 0.05 M KCl, using 500 msecond per second pulses of 1-3 nA depolarising current for 15-20 seconds. Only one ectoderm cell per embryo was injected, although occasionally two cells were labelled owing to the passage of the dye between mitotic pairs still connected by a cytoplasmic bridge (Lawson et al., 1991; Gardner and Cockcroft, 1998). An additional injection for 5 seconds was made into an extra-embryonic visceral endoderm (VE) cell near the embryonic/extra-embryonic junction and in the same focal plane as the injected ectoderm cell. The radial position of the resulting compact VE clone relative to the midline multiplied by the value for 25% of the circumference was used to define, retrospectively, the circumferential position (CX) of the injected ectoderm cell. The circumference was calculated using the mean diameter of the ectoderm layer at the level of the embryonic/extra-embryonic junction from longitudinal and frontal views. HRP-labelled cells were identified in cultured embryos after staining, fixation in 4% paraformaldehyde, ethanol dehydration and clearing in BABB (1:2 benzoyl alcohol:benzyl benzoate), before embedding in epoxy resin (Agar 100, Agar Scientific). Serial sections cut at 6 μm were recorded using DIC optics; images of those with HRP-labelled cells were stacked manually to count the cells and assess their position.

Plotting and visualisation of clones in 3D and creation of a 2D flat map

The procedures for the preparation and reconstruction of 1 μm frontal serial sections of the head of the cultured embryo used to plot the clones in 3D can be found at http://www.emouseatlas.org/emap/ema/home.html (EMA Anatomy Atlas/EMA Protocols and TS12/EMA:145). The Woolz image processing system (Piper and Rutovitz, 1985) was used. Anatomical and clonal cell domains were defined within the reconstruction using a combination of non-interactive image processing tools (grey level thresholding and morphological operations) and MAPaint (Baldock, 2004) for interactive voxel labelling and for identifying the sectioning plane in experimental embryos.

Triangulated mesh surface models were created corresponding to all the defined domains, and a simple affine scaling transformation was used to achieve an isotropic 1 μm voxel size. The mesh was cropped, smoothed and remeshed to produce a simply connected open surface (as required for parameterisation) using a combination of Woolz and MeshLab (Cignoni et al., 2008). A mesh-based transform was established between the cropped ectoderm surface mesh and its cropping plane. The mesh node displacements were computed using least squares conformal mapping with boundary nodes fixed to the cropping plane. The transformation was defined using least squares conformal parameterisation (Levy et al., 2002). The mesh transform defined a bi-directional mapping between the ectoderm surface and the planar flat map. Barycentric interpolation within mesh elements allowed the transformation of arbitrary positions between the 3D surface and 2D flat map. The parameterisation resulted in large variations in scale within the flat map, which made the distribution of clone cells hard to interpret. Fixed size circular markers were placed at their location to overcome this problem. A full description of the procedure will be published elsewhere. The clone cells, the ectoderm and other anatomical domain surfaces were visualised using VTK (Schroeder et al., 2007).

Calculation of clone and population expansion

Clonal growth is assumed to be exponential; then $N=N_0{}^{bt}$ or $\ln N=bt+\ln N_0$, where N is the number of labelled cells at time t (hours after injection), N_0 is the number of progenitors (1, or 2 when siblings were initially labelled). Clone doubling time (cdt) is given by $\ln 2/b=\ln 2\times t/\ln N-\ln N_0$.

The number of population doublings (n) in the targeted region is estimated by $2^n=\Sigma N/\Sigma N_0$, or $n=\ln\Sigma N-\ln\Sigma N_0/\ln 2$, where ΣN is the total number of labelled cells in all embryos with label after culture and ΣN_0 is the total number of labelled progenitors in these embryos.

Whole-mount in situ hybridisation (WISH) and histology

WISH and histology were performed as described (Perea-Gomez et al., 2004), using antisense probes from published sources (see Results). Embryos were cryosectioned at 20 μm.

RESULTS

Labelling single anterior ectoderm cells using iontophoresis

In order to trace cell lineage shortly before neural plate formation, single ectoderm cells of LS and LSEB stage embryos were microinjected by iontophoresis with a mixture of HRP and LRDX. The region targeted in the embryonic ectoderm covered the anterior midline, from the attachment of the amnion to the embryonic ectoderm, proximally to half of the distance to the node along the anterior midline, distally (distance PD; Fig. 1A). Laterally, the targeted region extended over 25% of the ectoderm circumference spanning the midline. The fluorescent label was used to immediately visualise the position of the injected cell (Fig. 1B; see Materials and methods) and HRP to identify its descendants after 1 day of culture (mean 24.7 hours, range 20.2-28.0 hours). Embryo development was coordinated normally, as judged by heart and neural morphogenesis and somite number [3-11 somite pairs, mean 5.60±1.85 (mean±s.d.)]. Of 93 single-cell-injected embryos, 58 (62%) had HRP-labelled descendants after culture. Of these, 47 were labelled in ectoderm, eight in mesoderm and three in endoderm. The clones in the last two categories were identified as the descendants of mesoderm and endoderm cells accidentally impaled instead of ectoderm and were not considered further. Informative histological sections were obtained from 41 of the embryos with ectoderm clones. Their analysis forms the basis of this study.

Clone size and doubling time

The frequency distribution of clone size (Fig. 1C) showed peaks at four, eight and 16 cells, indicating some synchronisation of the cell cycle (Lawson et al., 1991; Tzouanacou et al., 2009). The clones in seven embryos were derived from two labelled siblings (see Materials and methods). These clones fell into two groups in the distribution: the four largest clones, and three clones with no more

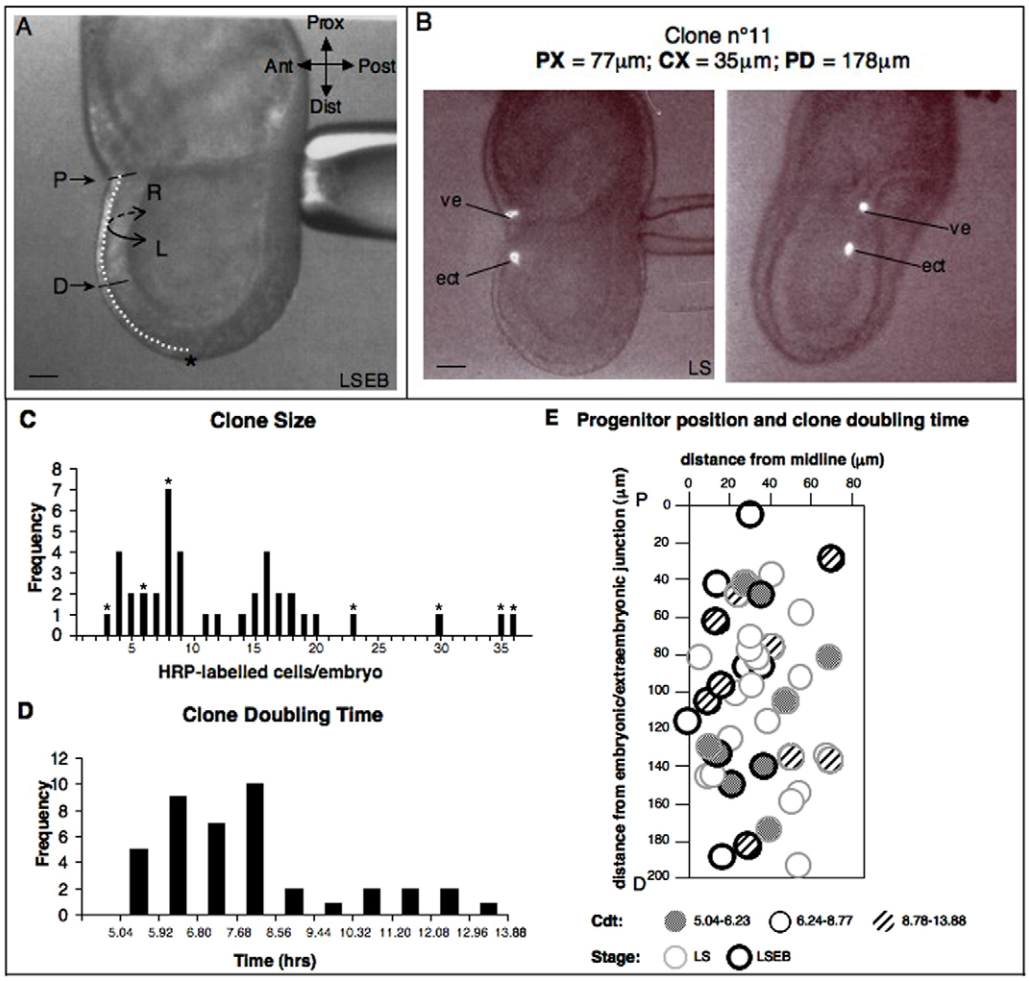

Fig. 1. Clone initiation and clone expansion. (**A**) The region studied by clonal analysis extends along the anterior midline from the embryonic/extra-embryonic junction (P) to a point (D) halfway to the node (asterisk). Measurements along the sagittal contour of the ectoderm (white dotted line) gave a PD mean of 180±13 µm (±s.d.). Laterally, the injections encompassed 25% of the circumference of the ectoderm spanning the midline (curved arrows). The mean left-to-right distance (LR) was 192±40 µm. (**B**) Lateral (left) and frontal (right) views of a mouse embryo just after injection. Fluorescence marks the position of one ectoderm cell (ect) and one visceral extra-embryonic endoderm cell (ve). The coordinates of each injected ectoderm cell are defined by the longitudinal (PX) and the circumferential (CX) positions and the size of the embryo is shown by the PD value. The nominal error for PX is ± 5 µm and that for the retrospectively estimated CX is ± 25 µm (see Materials and methods). (**C**) Frequency distribution of the number of HRP-labelled cells per embryo (clone size) after 1 day of culture. Asterisks indicate that one clone originated from two siblings. (**D**) Frequency distribution of the clone doubling time (cdt). (**E**) cdt and initial developmental stage related to progenitor position. The origins of both abscissa and ordinate correspond to P. Left and right sides are superimposed. The fastest and slowest expanding clones (outside 99% confidence limits of the median) are indicated with shading and hatching, respectively. There is no obvious difference between the distribution of labelling sites in late streak (LS) and late streak/early bud (LSEB) stage embryos. Scale bars: 50 µm in A; 62 µm in B.

than eight labelled cells. For the latter group, the clone doubling time (cdt) was calculated on the basis of one surviving sibling (see Materials and methods). The total number of labelled cells (509) from 45 progenitors (37 singletons and four doublets) implies an 11.4-fold increase in the size of the targeted population, or 3.5 population doublings. The cdt showed a skewed distribution with median 7.65 hours and 95% confidence limits 6.91 and 8.17 hours (Fig. 1D). Clones with a very long or very short cdt were examined for spatial clustering that could indicate a lengthening of the cell cycle accompanying early differentiation on the one hand, or a local area of very rapid proliferation on the other. Progenitors of both groups were scattered throughout the targeted area (Fig. 1E), indicating that the anterior ectoderm comprises a uniformly proliferating population.

Clone composition and progenitor position

Anatomical boundaries, cell shape and cell arrangement were used to score descendant cells as belonging to the neural primordium or to one of three distinguishable regions of the non-neural ectoderm: the ectoderm in contact with the overlying anterior prosencephalon neuroectoderm layer, without intervening mesoderm (VEAP for 'ventral ectoderm of the anterior prosencephalon'); the buccal ectoderm (oral or stomodeum epithelium); and the surface ectoderm (Fig. 2A,B). The buccal ectoderm, which includes the oral plate, is a cuboidal epithelium that is continuous with the VEAP and extends to the squamous surface ectoderm covering the heart. Examples of labelled cells in neural or non-neural ectoderm derivatives are shown in Fig. 2C-G.

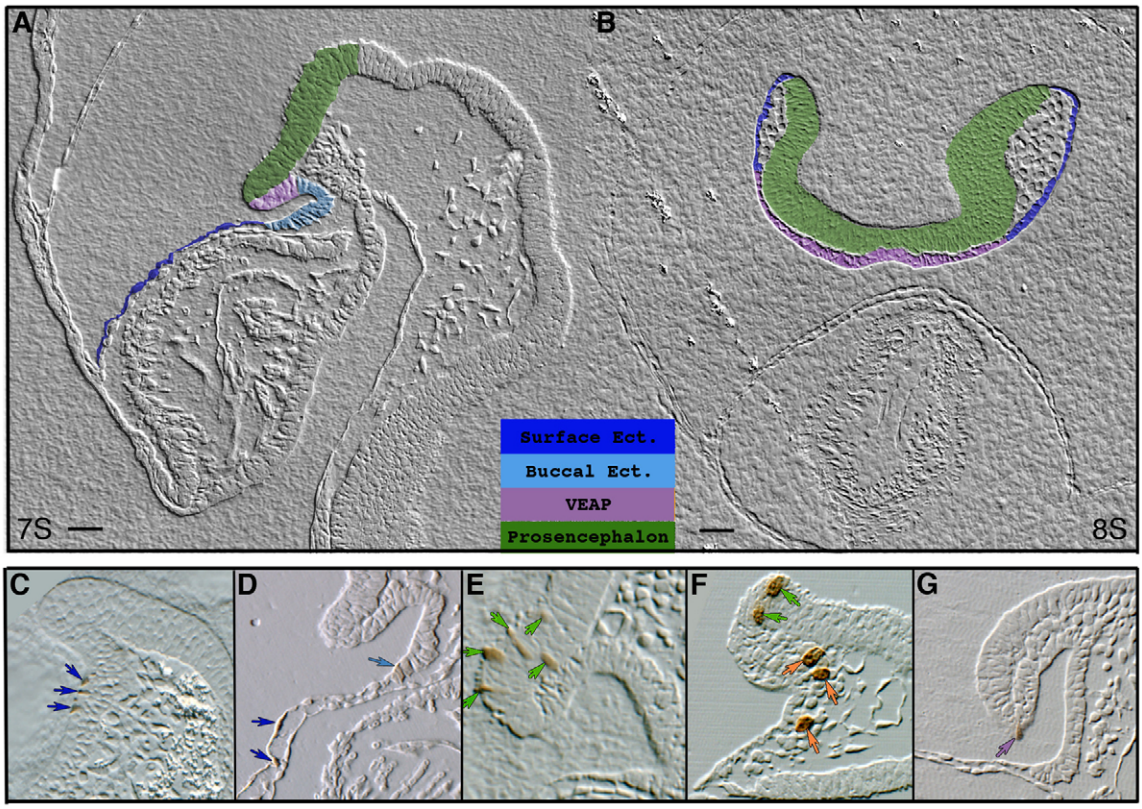

Fig. 2. Histological sections showing HRP-labelled cells after 1 day of culture. (**A**,**B**) Parasagittal (A) and frontal (B) sections of cultured mouse embryos showing painted anatomical domains colonised at E8.5 (7- or 8-somite stage). (**C-G**) Longitudinal (D,E,G) and frontal (C,F) histological sections with examples of contribution to (C,D) surface ectoderm (dark-blue arrows), (D) buccal ectoderm (light-blue arrow), (E,F) forebrain neuroectoderm (green arrows), (F) emigrating neural crest cells at the level of the forebrain (orange arrows) and (G) ventral ectoderm of the anterior prosencephalon (VEAP; purple arrow). Scale bars: 25 μm in A; 30 μm in B.

A pie chart spatial representation (Fig. 3) shows the original positions of clone progenitors and the tissue contributions of their respective descendants. We were able to identify a proximal region that did not contribute to the forebrain. The most proximal forebrain progenitor was 77 μm from the embryonic/extra-embryonic junction (or 0.43 when normalised to PD length) and established the limit for forebrain contribution (LFBC) (Fig. 3). By contrast, contribution to non-neural ectoderm was found throughout the targeted area. However, progenitors further than 106 μm from the embryonic/extra-embryonic junction (0.56 normalised) contributed to the VEAP exclusively or in combination with neuroectoderm, but not to buccal or surface ectoderm. A limit for surface ectoderm contribution (LSEC) was thus defined (Fig. 3). We therefore distinguished three zones along the anterior midline: a proximal zone (PROX), a distal zone (DIST) and, in between, an intermediate zone (INT) delineated by the LFBC and LSEC (Fig. 3). With the exception of two labelled cells in the hindbrain, all descendants of the PROX zone clone progenitors colonised the surface ectoderm and buccal ectoderm (Table 1, Fig. 3). By contrast, 88% of the descendants of the DIST zone clone progenitors populated the neuroectoderm, with a majority in the forebrain (Table 1, Fig. 3); the remaining 12% were in the VEAP (Table 1). The INT zone was characterised by progenitors that generated a wide variety of fate combinations, diversely associating all neural and non-neural fates described for the PROX and DIST zone progenitors (Table 1, Fig. 3). These results show that, at late gastrulation stages, the anterior ectoderm exhibits a significant regionalisation of prospective fate and a marked segregation of neural and non-neural progenitors.

Clones yielding exclusive colonisation of neuroectoderm derivatives (15/41) originated from the INT and DIST zones. By contrast, labelled progenitor cells showing descendants exclusively in non-neural derivatives (16/41) were found over the entire anterior ectoderm. For these progenitors, a clear correlation was observed between their original location and the specific non-neural structure to which they contributed (Fig. 3). Nevertheless, a number of progenitors contributed to both neural and non-neural structures (10/41). Among these progenitors, two types could be distinguished: mixed fate progenitors confined to the INT zone (5/10) that generated an array of neural and non-neural fate combinations; and mixed fate progenitors from the DIST zone (4/11) that consistently generated descendants contributing to the forebrain and the VEAP. Together, these findings demonstrate that neural and non-neural fates are regionalised but not clonally separated. Some descendants in the VEAP, which is continuous with the buccal and surface ectoderm at E8.5, are clonally related to neural precursors.

Dynamic patterns of anterior gene expression during neural plate formation

We investigated possible links between the regionalisation of prospective cell fate and the expression patterns of anterior-specific genes. We examined the spatial and temporal evolution of both

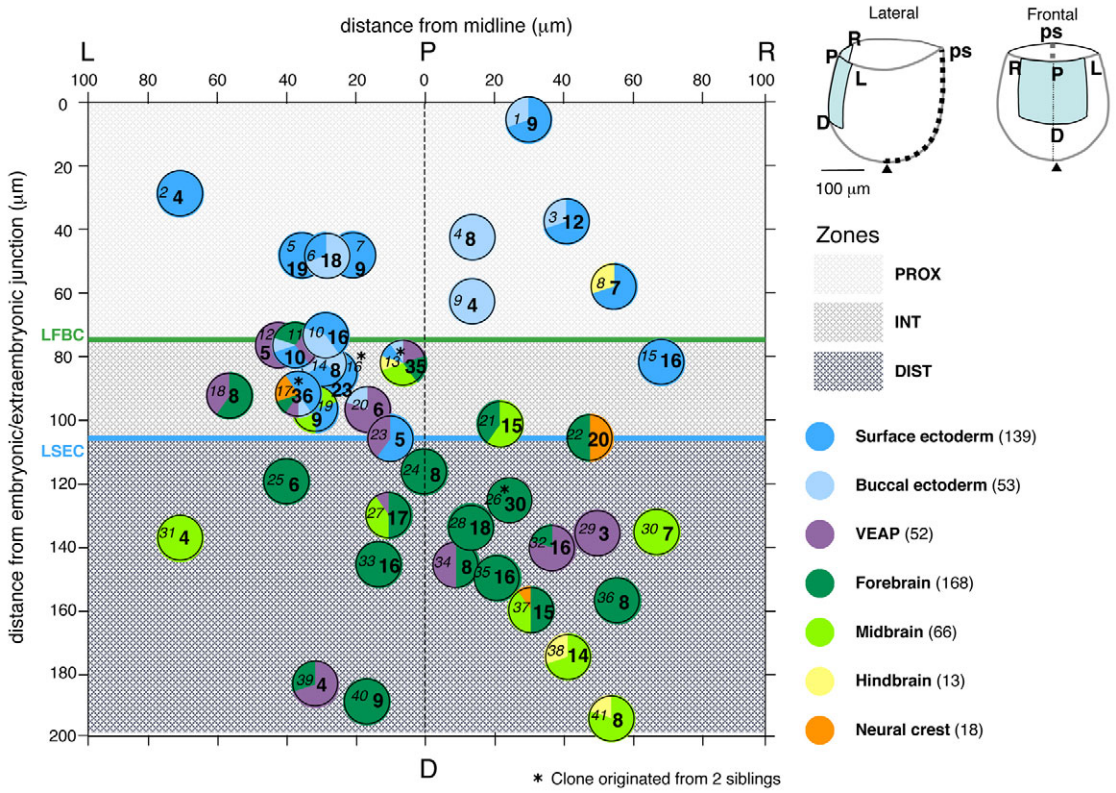

Fig. 3. Tissue contributions of descendant cells according to the original position of HRP-injected progenitors. Note that the plotted area has been derived from the curved basal surface of the ectoderm (see Fig. 1A) and, compared with a projection, is 7% greater in the proximodistal direction (most of the curvature being in the distal half of the embryo) and ~11% in the left-right direction. The plotted area is represented in blue in the upper right schematics. The pie charts and colour codes show the relative composition of each clone to the nearest 10%. The centre of the circle corresponds to the position of the clone progenitor. The clone identification code (in italics) and total descendant number (in bold) are indicated. The green line marks the rostral limit of forebrain contribution (LFBC) and the blue line marks the caudal limit of surface ectoderm contribution (LSEC). The total number of HRP-labelled cells found in each derivative is in parentheses. Zones PROX, INT and DIST are described in the text.

lineage-specific markers and regional markers: *AP-2.2* (*Tfap2c* – Mouse Genome Informatics) and *Dlx5* [non-neural ectoderm (Chazaud et al., 1996; Yang et al., 1998)], *Sox1* [neuroectoderm (Pevny et al., 1998)], *Sox2* [neuroectoderm and surface ectoderm precursors (Avilion et al., 2003)], *Hesx1* and *Six3* [prospective forebrain (Thomas and Beddington, 1996; Yang and Klingensmith, 2006)], *Otx2* [prospective forebrain and midbrain (Ang et al., 1994)] and *Irx3* [posterior forebrain, midbrain and hindbrain (Kobayashi et al., 2002; Braun et al., 2003)].

Analysis of expression patterns from LS to late headfold (LHF) stage (Downs and Davies, 1993) revealed several unreported features (Fig. 4). *Six3* and *Sox1* were expressed at LSEB stage, earlier than previously reported. Both transcripts were found at the same axial level, just rostral to the node (Fig. 4D,F, compare with *Gsc* and *Foxa2* in supplementary material Fig. S1), but the *Sox1* domain was broader, extending laterally, and no *Sox1* transcript was detected in the midline. Strikingly, *Six3* ectodermal expression started at a very distal position compared with *Hesx1* expression at the same stage (Fig. 4C,D). Later, *Six3* expression spread rostrally and slightly laterally and, by early headfold (EHF) stage, colocalised with *Hesx1* expression. *Irx3* transcripts were first detected at LS stage, lateral to the *Six3* domain. Later, the two expression domains overlapped although *Irx3* expression appeared weaker where *Six3* was expressed. *AP-2.2* transcription was consistently weaker than that of *Dlx5* and clearly absent from ectoderm cells of the anterior midline (Fig. 4A,B). This analysis highlights dynamic changes in exclusive and overlapping domains of ectodermal gene expression during early embryonic development.

Table 1. Distribution of HRP-labelled cells in neural and non-neural derivatives according to PROX, INT and DIST zones

		Non-neural derivatives (244)				Neural derivatives (247)					
Injected zone	No. of clones	Surface ectoderm	Buccal ectoderm	VEAP	Subtotal	Forebrain neuroectoderm	Midbrain neuroectoderm	Hindbrain neuroectoderm	Subtotal	NCCs	Total descendants
PROX	10	67	37	0	104	n.a.	0	2	2	0	106
INT	13	72	16	27	115	34	26	5	65	16	196
DIST	18	n.a.	n.a.	25	25	134	40	6	180	2	207
Total	41	139	53	52		168	66	13		18	509

The total number of cells in non-neural and neural derivatives is indicated in parentheses.
n.a., not applicable.

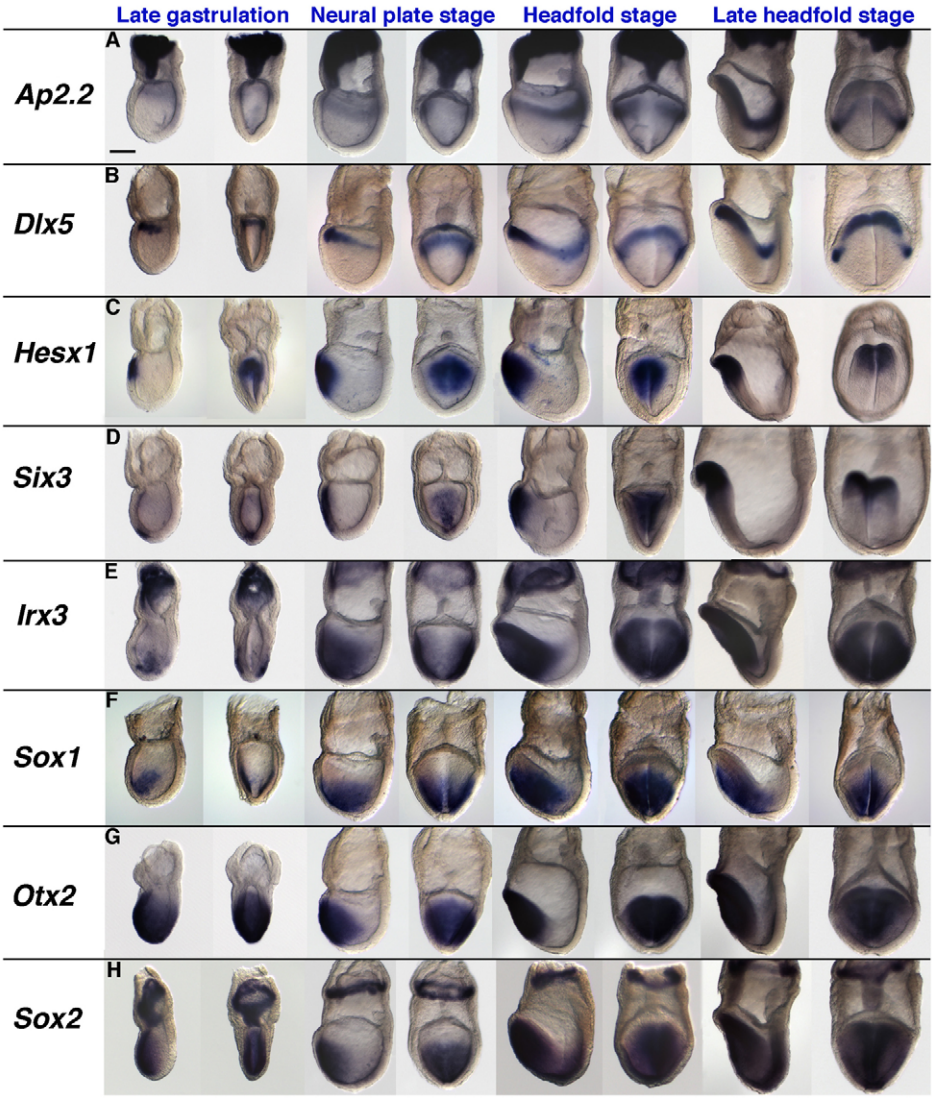

Fig. 4. Temporal and spatial expression of anterior regional markers and lineage-specific markers from LS to late headfold (LHF) stages. The expression patterns of (**A**) *AP-2.2* (*Tfap2c*), (**B**) *Dlx5*, (**C**) *Hesx1*, (**D**) *Six3*, (**E**) *Irx3*, (**F**) *Sox1*, (**G**) *Otx2* and (**H**) *Sox2* are shown on lateral and frontal views (left and right, respectively, of each pair). Note that *Six3* is first detected in the axial mesendoderm and the adjacent ectoderm cells (D). Scale bar: 170 μm.

Cartography of the anterior expression patterns and correlation with the fate map

The proximal and distal expression boundaries of the *Dlx5*, *Hesx1*, *Sox1* and *Sox2* genes were defined along the anterior midline to establish how they relate to cell fate. These are classical markers of anterior, non-neural and neural identities. Only LS to late bud (LB) stage embryos were analysed as developing headfolds prevented measurements. Actual values of the expression boundaries were plotted against embryo size (Fig. 5). At all stages examined, the rostralmost gene was *Dlx5* with, slightly caudal to it, *Hesx1*. The *Sox2* proximal boundary coincided early on with the *Hesx1* proximal boundary. By contrast, when *Sox1* was first detected, its proximal boundary of expression abutted the *Hesx1* distal boundary (Figs 4, 5). Normalised values indicate that *Sox1* expression expands anteriorly as the embryo grows (data not shown). *Sox1* and *Dlx5* expression domains were mutually exclusive at all stages examined. Two phases could be distinguished: an early phase from LS to EB (PD=160-200 μm), when the *Hesx1* and *Dlx5* expression domains overlap rostrally, is followed, from EB to LB (PD=200-300 μm), by the onset of *Sox1* expression, the domain of which progressively overlaps that of *Hesx1* caudally. At all stages examined, a significant area of the anterior ectoderm positive for *Hesx1* remained negative for both the non-neural marker *Dlx5* and the neural marker *Sox1*.

We compared the positions of the LFBC and LSEC defined in the fate map with gene expression boundaries at equivalent stages (Fig. 5). The PROX zone that contributes to both surface and buccal ectoderm lay within a domain in which *Dlx5* is expressed alone or is co-expressed with *Hesx1*. The mixed progenitors confined to the INT zone were located just distal to the *Dlx5* domain and, like the progenitors of the DIST zone contributing to forebrain and VEAP, were in a region of ectoderm expressing *Hesx1* exclusively. Together, these results demonstrate that, at E7.5, markers of forebrain, neuroectoderm and surface ectoderm do not define lineages. However, their collective expression defines ectoderm subdomains that correlate with areas showing distinct prospective fates.

Three-dimensional representation of clone expansion

The anterior ectoderm undergoes substantial growth and complex morphogenetic curvature during early neurulation. In order to gain insight into this process we analysed the clone spatial distribution

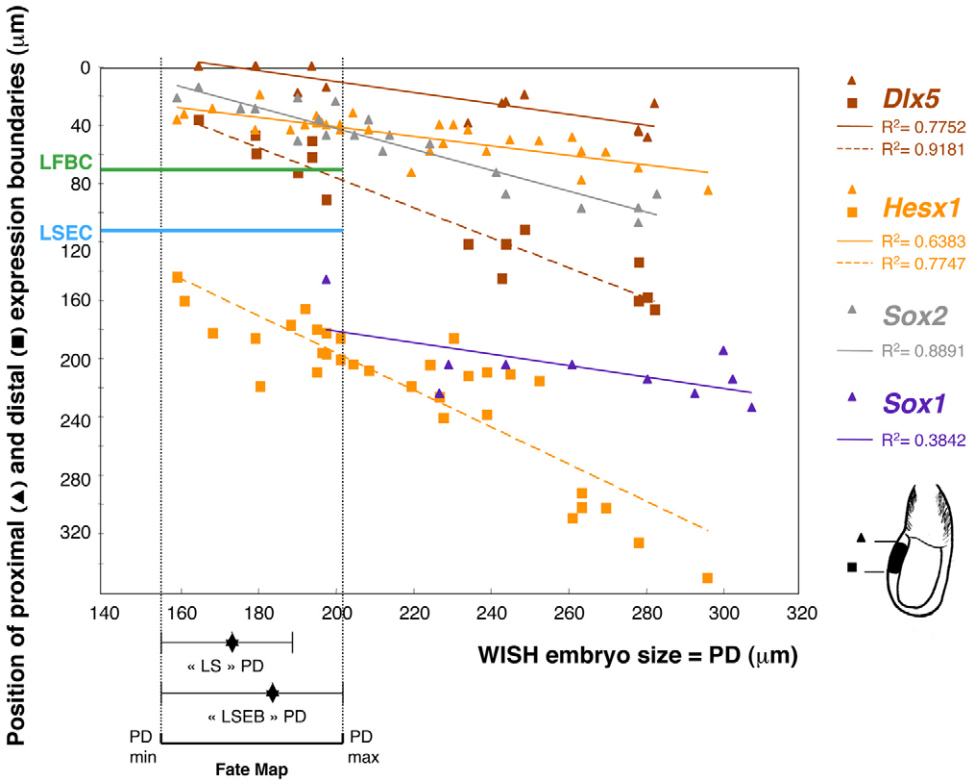

Fig. 5. Relationship between gene expression patterns and the prospective fate map. The distance from the embryonic/extra-embryonic junction of the proximal (triangles) and distal (squares) expression boundaries of *Dlx5* (*n*=15 embryos) and *Hesx1* (*n*=32) plotted against embryo size as reflected by PD, for LS to LB stages (see Fig. 1A). The positions of the proximal expression boundaries of *Sox2* (*n*=20) and *Sox1* (*n*=10) are also shown. Note that *Sox1* expression is absent in younger embryos (PD<200 μm). Each point represents an individual embryo. Colour-coded lines represent the linear regression of each point set. Correlation coefficients indicate a significant statistical relationship between the gene expression boundaries and embryonic size (*P*<0.001). The PD mean and range values of the fate map experiment (horizontal dashed lines) and the positions of LFBC and LSEC are indicated (green and blue lines). Together, they delimit an area that corresponds to the INT zone, which is composed of mixed fate progenitors. Values were adjusted for 5.6% shrinkage in PD in the WISH-treated embryos.

using a high-resolution 3D reconstruction of the head of a 5- to 6-somite stage embryo, cultured from the LSEB stage (supplementary material Fig. S2). Cells occupying positions that matched those of the labelled cells in sections were painted in the reconstruction, enabling a representation of the position and general orientation of the clones. Anatomical domains were also painted in the reconstruction. The ectoderm layer was then extracted as a 3D surface with the associated painted cells and anatomy (Fig. 6A-E). The clone spatial distribution could be viewed from any angle (supplementary material Movie 1) and plotted clones checked against the record of clones in the intact embryo (Fig. 7). In order to compare with published data on other species, the 3D surface was transformed into a flat map (Fig. 8A; supplementary material Fig. S3 and Movie 1).

In practice, only 24 embryos had sufficient congruency for matching into the reconstruction. Most of these embryos had 5-8 somites and had been injected at a significantly more advanced stage (9 at LS, 15 at LSEB) than the remaining embryos (15 at LS, 2 at LSEB; χ_c^2=10.14, 1 degree of freedom, P<0.005). Neural clones from the latter group consistently showed extension into midbrain and even into anterior hindbrain ('not-plotted' clones), indicating that caudal extension from the prospective forebrain region starts to decrease sometime between the LSEB and early somite stage. Other not-plotted clones were included in the description when their distribution could be grouped with plotted clones that had similarly situated progenitors.

The following description of clone expansion is based on the three zones that have been distinguished by their clonal composition. During gastrulation, clones from anterior epiblast are non-coherent and anisotropic, typically expanding towards the PS, i.e. aligned approximately parallel to the embryonic/extra-embryonic junction (Lawson et al., 1991). The behaviour of clones generated in the PROX zone shortly before neural plate formation followed this pattern (Fig. 8A,B): clones in buccal and surface ectoderm were either elongated laterally away from the midline (clones 3, 4, 6 and not-plotted 9), or had colonised the surface ectoderm at the level of the midbrain and anterior hindbrain, leaving no descendants in buccal ectoderm (clones 2, 5, 7). Clone 1 was an exception: initially labelled very close to the embryonic/extra-embryonic junction, it extended parallel to the midline as squamous ectoderm over the heart, ending in buccal ectoderm.

Clones generated in the INT zone showed a mixture of behaviours (Fig. 8A,C). Two clones (12, 20) spread laterally away from the midline in the VEAP. Four clones (14, 15, 16 and the caudal group of cells in 17) colonised some buccal ectoderm, but mainly surface ectoderm dorsal and generally rostral to the region occupied by clones 5 and 7 from the PROX zone. Three clones diverged from the expansion pattern typical of epiblast clones. They were confined, away from the midline, in the junctional region between forebrain, VEAP, buccal and surface ectoderm, oriented from surface ectoderm and buccal ectoderm through the

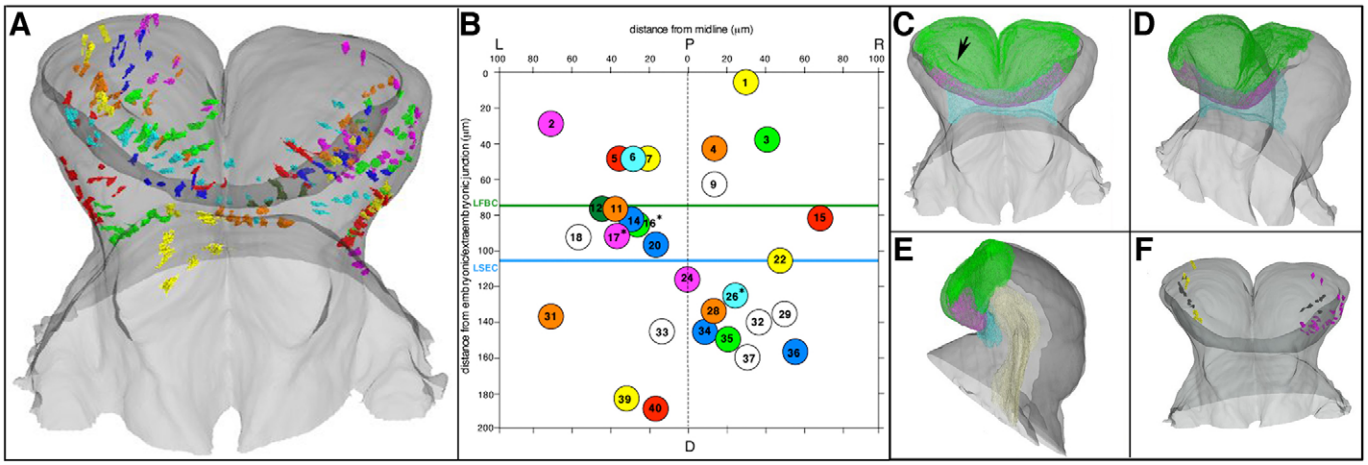

Fig. 6. Spatial distribution of the clones in a 3D reconstruction of the mouse embryo head. (**A**) Frontal view of all plotted clones in the extracted 3D surface of the ectoderm layer. (**B**) Proximodistal and left-right positions and colour-code for the progenitors of the clones displayed. White circles represent clones cited in the text but not plotted in the reconstruction. Asterisks indicate that one clone originated from two siblings. (**C-E**) Frontal (C), oblique (D) and left (E) views of the anatomical domains painted in the reconstruction: forebrain (green), VEAP (purple), buccal ectoderm (blue) and foregut endoderm (yellow). The arrow indicates the optic pit in the right headfold. (**F**) Representation of two plotted clones (clone 17 in magenta, clone 22 in yellow) contributing to emigrating neural crest cells (NCCs; grey-painted cells) at the forebrain level.

most caudal part of the VEAP and rostrally to neural (clone 11, not-plotted 18), or from VEAP slightly caudally through surface ectoderm to neural (rostral group of clone 17).

All plotted clones generated in the DIST zone contributed to the neuroectoderm, within which three types of behaviour could be distinguished (Fig. 8A,D). First, clones that spanned the midline (26, 40 and not-plotted 33) did so only anterior to the foregut, rostral to the nascent optic pit, and were presumably prospective telencephalon. Second, clones that were localised in the forebrain on the side on which they originated spread from the midline rostrally and laterally (clone 35), laterally and caudally (24, 28) or primarily caudally for the most lateral progenitors (22, 36), plus a small clone in the midbrain (31). Third, clones contributing to both neuroectoderm and VEAP (34, 39) were located in the VEAP further away from the midline than clones 12 and 20 from the INT zone and spread into the neuroectoderm near the junctional region between forebrain, VEAP, buccal and surface ectoderm, i.e. into a similar position as clone 11 from the INT zone. Of the two not-plotted clones contributing to the VEAP from the DIST zone, clone 29 was similar to clone 34 and clone 32 spread more widely throughout the left VEAP, extending into neural on the right side, and so showed elements of different behavioural categories. Importantly, whether a clone was localised in prospective telencephalon or diencephalon was not predictable from the proximodistal position of its progenitor. Therefore, we concluded that cells of the rostral neural boundary are not spatially organised at the end of gastrulation and the prospective forebrain territory is not regionally subdivided at this stage.

Contribution to neural crest cells (NCCs)

We identified putative NCCs (Fig. 2F) in two plotted clones (17, 22) from the INT zone and one not-plotted clone (37) from the DIST zone (Fig. 3), outside the presumptive *AP-2.2* expression domain (Fig. 4). Thus, at E7.5, the anterior limit of *AP-2.2* does not

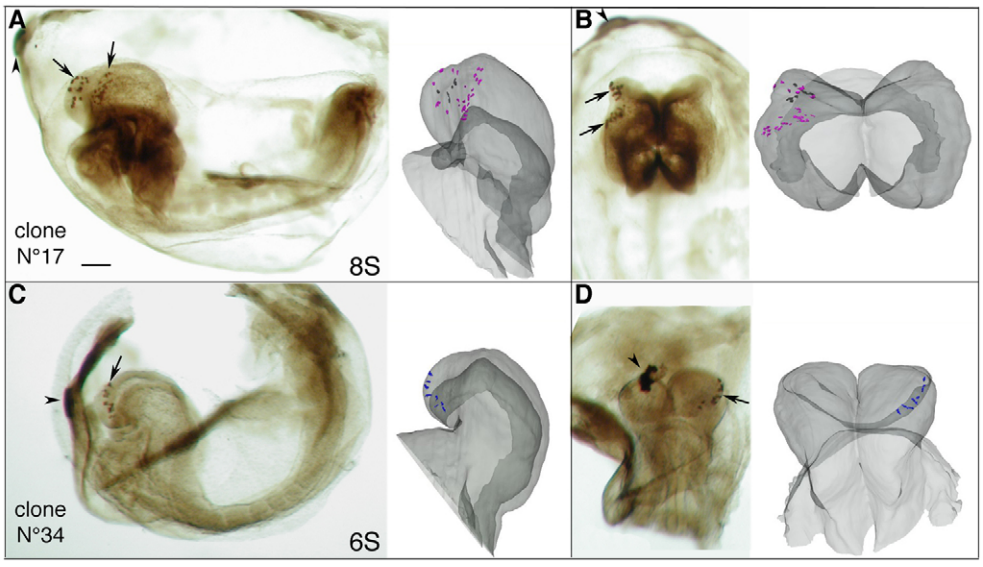

Fig. 7. Whole-mount images of HRP-labelled mouse embryos and corresponding representation of the clones plotted in the 3D reconstruction. (**A**,**B**) Lateral (A) and dorsal (B) views of clone 17 at the 8-somite stage showing two distinct groups of labelled descendant cells (arrows) in the left headfold. Each group presumably derives from one of the documented siblings. (**C**,**D**) Lateral (C) and frontal (D) views of clone 34 at the 6-somite stage showing labelled descendants in the neuroectoderm and the VEAP of the left headfold (arrows). Arrowheads mark the descendants of the injected visceral endoderm cell. Scale bar: 130 µm.

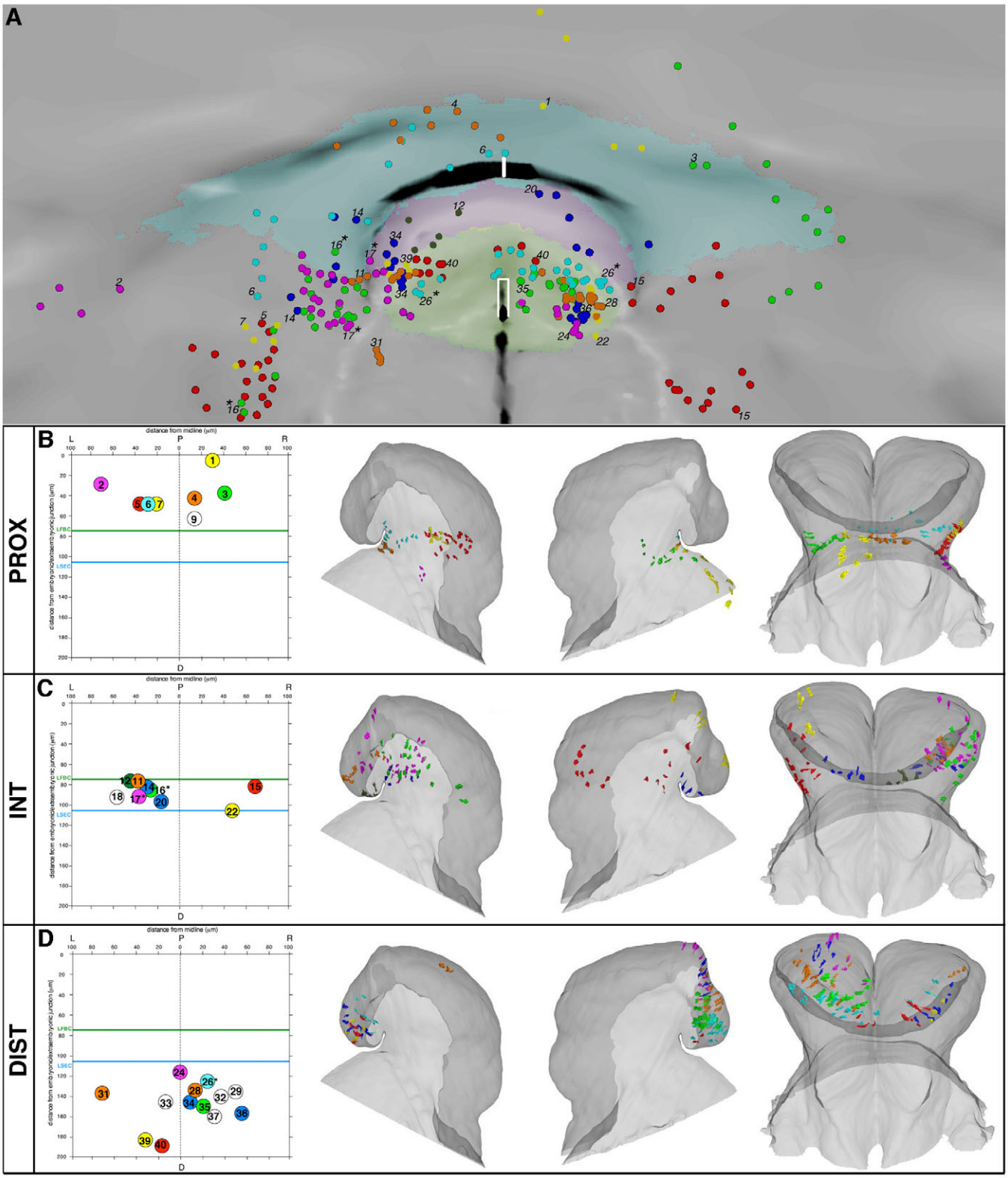

Fig. 8. Two-dimensional flat map and representation of clone dispersion. (**A**) Distribution of the painted clones and anatomical domains represented in a 2D flat map (dorsal view). Part of the whole 2D flat map (see supplementary material Fig. S3 for the whole flat map) has been magnified here. Anterior is at the top. Anatomical domains are only shown for prospective forebrain (green), VEAP (purple) and buccal ectoderm (blue). Clone identification and position at the time of labelling and associated colour code after 24 hours of culture are as in Fig. 6B. The white open-ended rectangle represents the midline position of the foregut and the white bar represents the position of the oral plate. (**B-D**) Clone spatial dispersions based on the PROX, INT and DIST zones that have been distinguished by their clonal composition. Rows show the spatial position and colour code of the plotted progenitors and then left, right and frontal views of the 3D reconstruction. Asterisks indicate that one clone originated from two siblings.

define the rostral limit of NCC production (Osumi-Yamashita et al., 1994). In support of previous ultrastructural (Nichols, 1981) and DiI-labelling (Serbedzija et al., 1992) studies of cranial NCCs in the mouse embryo, we found emigrating NCCs at the level of the forebrain (clones 17, 22), located caudal to the optic pit (Fig. 6F) and in the mesencephalon (clone 37).

ANR precursor distribution and lineage relationships

To characterise the molecular identity of the tissues generated by anterior ectoderm cells at E8.5 and to determine which clones had descendants in the ANR, we compared the expression profiles of *Six3*, *Hesx1*, *Foxg1*, *Dlx5* and *Fgf8* (Oliver et al., 1995; Xuan et al., 1995; Thomas and Beddington, 1996; Yang et al., 1998; Hatini et al., 1999). Longitudinal and frontal histological sections were obtained from 3- to 7-somite stage embryos ex utero stained by WISH (Fig. 9A-P; data not shown). In the mouse embryo, the ANR is located at the junction between the most rostral part of the neural plate and the non-neural ectoderm; it expresses *Fgf8* from the 4-somite stage onward (Shimamura and Rubenstein, 1997), so it comprises both forebrain and VEAP cells at the anatomical anterior ridge (Fig. 9M-O′). The overlap between the *Dlx5* and *Fgf8* expression domains corresponds to the non-neural, i.e. VEAP, part of the ANR (Fig. 9J-L′).

Information about the *Fgf8* expression domain was used to locate the presumed ANR in sections of the HRP-labelled embryos. Thirteen clones had descendants in the ANR. The progenitors were scattered throughout the INT and DIST zones (Table 2, Fig. 2G, Fig 9Q). Four clones had labelled cells only in the ANR: two clones generated in the INT zone (12, 18) and two in the DIST zone (34, 39). About half of the progenitors contributing to the ANR also had descendants spreading widely in the forebrain (six out of 13). Interestingly, three of those originating in the DIST zone (clones 26, 27, 40) had descendants in the ANR and the forebrain only (Fig. 9Q). Consistent with the observation that the INT zone is characterised by progenitors with a variety of fate combinations, four out of six clones with descendants contributing to the ANR (11, 13, 20, 23) also showed colonisation of neuroectoderm, buccal ectoderm and surface ectoderm. Together, these findings demonstrate that prospective ANR cells arise from progenitors that are distributed over a broad area of the anterior ectoderm and interspersed with precursors of other tissues. Furthermore, these findings reveal that, clonally, prospective ANR cells are more closely related to forebrain than to non-neural tissues.

DISCUSSION

Organisation of the progenitors and molecular regionalisation at the end of gastrulation

In agreement with previous fate map studies, we found that anterior ectodermal cells differentiate into neuroectoderm, epidermis and intermediate cell types characteristic of the border between the neural plate and non-neural ectoderm. However, our findings diverge with regard to other tissue contributions. A previous report showed that a small fraction of the descendants of anterior ectoderm grafts colonised cranial mesenchyme and heart mesoderm (Tam, 1989). A retrospective analysis of genetically labelled single cells showed that common neuromesodermal progenitors persist long after the segregation of endoderm and surface ectoderm lineages, which occurs during gastrulation (Tzouanacou et al., 2009; Petit and Nicolas, 2009). We found no contribution to mesoderm, indicating that, if present, neuromesodermal progenitors are rare within the anterior part of the embryo at E7.5. This strongly suggests that lineage segregation occurs earlier anteriorly than for caudally and laterally located progenitors. Nevertheless, restricted cell fate is not a demonstration that these cells have lost the potential to differentiate into mesoderm (Chan and Tam, 1986).

Previous studies using orthotopic grafts showed that, although non-neural and neural precursors are intermingled, a rostrocaudal organisation of forebrain, midbrain and hindbrain neuroectoderm precursors could be distinguished at E7.5 (Beddington, 1981; Beddington, 1982; Tam, 1989). The higher resolution provided by clonal analysis revealed a tendency for the anterior midline cells to be restricted in their prospective fate and showed that their spatial segregation is also well underway. Proximal ectodermal progenitors expressing *Dlx5* contributed to surface and buccal ectoderm, whereas progenitors located more distally and expressing *Hesx1* predominantly contributed to the neuroectoderm and the VEAP. Together, our findings establish that neural and non-neural lineages are not yet clonally separated at E7.5. Importantly, our revised fate map delineates a rostral limit, beyond which no forebrain contribution is found, at a position that is more distal, i.e. farther from the embryonic/extra-embryonic junction than that previously reported.

Three-dimensional reconstruction allowed us to visualise cell dispersion and the mode of clonal growth in the anterior cephalic region. The behaviour of clones generated in the proximal ectoderm shortly before neural plate formation followed the lateral and caudal expansion expected from epiblast cells at earlier stages. By contrast, for more distally located ectoderm cells, in particular for forebrain and VEAP progenitors, different combinations of cell behaviours were observed. No correlation between the anteroposterior position of these progenitors and the subsequent dispersion patterns of their descendants was observed. These findings lead us to conclude that the anteriormost border of the neural plate is not spatially defined at the end of gastrulation, nor is there early regional subdivision of the prospective forebrain territory. Therefore, the organisation of the mouse embryo appears to differ from that of the zebrafish (Mathis and Nicolas, 2006). Late in gastrulation, discernible domains in the zebrafish dorsal blastoderm can be assigned to major subdivisions of the forebrain (Woo and Fraser, 1995), which resembles the neural fate map of *Xenopus* (Eagleson and Harris, 1990) and chick (Couly and Le Douarin, 1985; Cobos et al., 2001).

In line with molecular evidence of anterior ectoderm regionalisation at the end of gastrulation, patterns of cell behaviour demonstrate significant regionalisation in prospective fate. However, overlapping regions of transcription factor expression often persist until LHF stage. Together, these findings demonstrate that molecular regionalisation and, in particular, classical surface ectoderm and forebrain markers, do not strictly define lineages at late gastrulation stage. In the mouse, the establishment of strict clonal boundaries appears to be a later event that could arise by progressive restriction of cell dispersion, rather than by a process of lineage specification, resulting from distinct combination of prepattern factors (Fraser et al., 1990; Inoue et al., 2000; Mathis and Nicolas, 2002; Puelles et al., 2005; Veitia and Salazar-Ciudad, 2007).

Pool of mixed fate precursors: potential roles in forebrain development

Our results reveal the existence of a distinct population of precursor cells that generates a wide range of neural and non-neural fate combinations. Strikingly, these mixed fate progenitors are confined to a small area of the anterior midline, the INT zone, delineated by the LFBC and the LSEC. It is interesting to compare these findings with data obtained in other vertebrate models. FGF, WNT and BMP

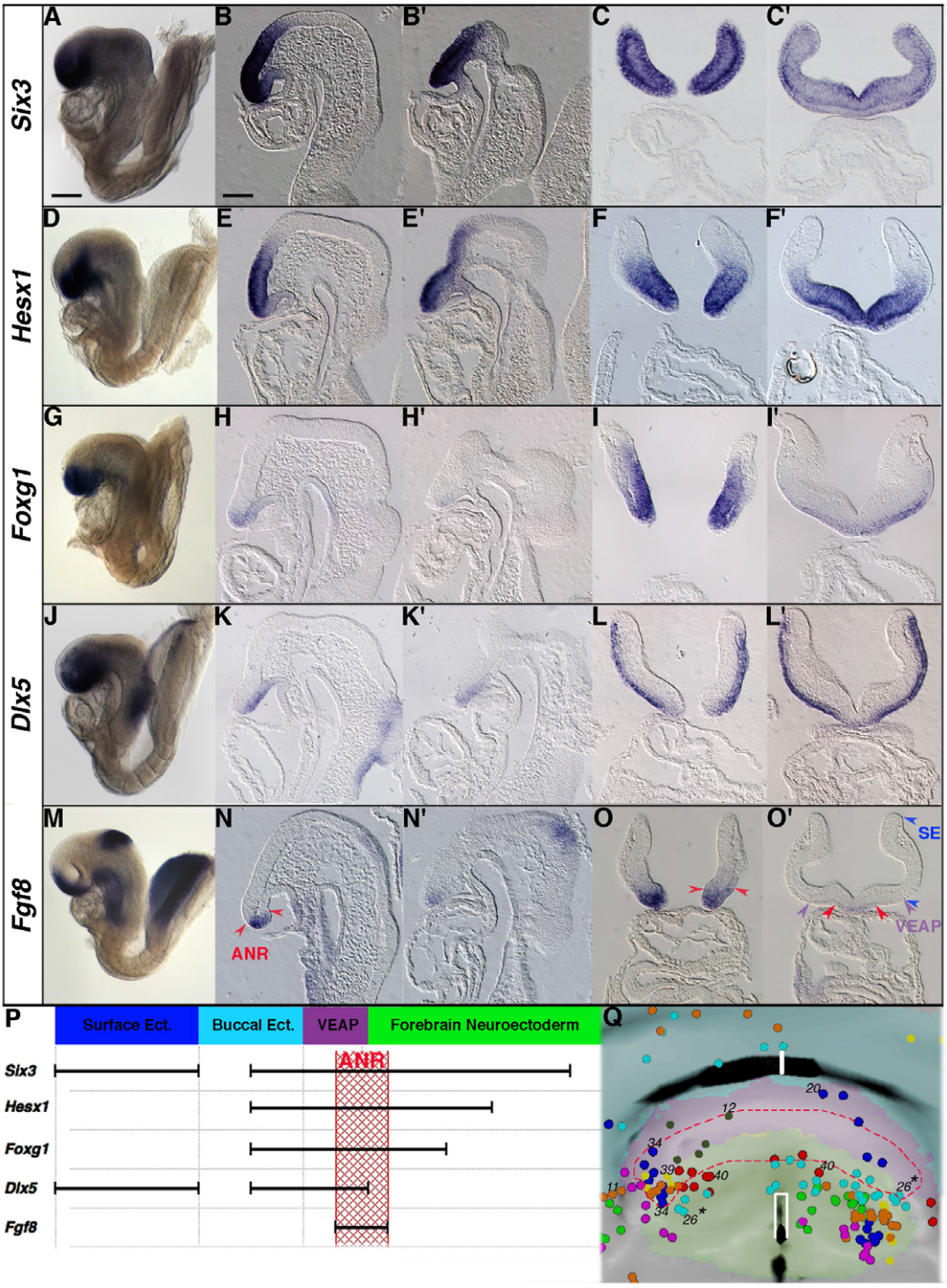

Fig. 9. Molecular analysis of the non-neural and neural tissues forming the rostral end of the head. (**A-O'**) Whole-mount (A,D,G,J,M), parasagittal (B,E,H,K,N), sagittal (B′,E′,H′,K′,N′) and frontal (C,C′,F,F′,I,I′,L,L′,O,O′) histological sections of 5- to 7-somite stage embryos. (A-C′) *Six3* is strongly expressed throughout the forebrain neuroectoderm, the VEAP, the buccal ectoderm and the surface ectoderm. (D-F′) *Hesx1* is strongly expressed in the forebrain but weakly in the VEAP and the buccal ectoderm. (G-I′) *Foxg1* is expressed in the forebrain, the VEAP and the buccal ectoderm. (J-L′) *Dlx5* is expressed in the VEAP, the buccal ectoderm and the surface ectoderm. (M-O′) *Fgf8* expression is found in the anterior neural ridge (ANR) and the isthmus at the midbrain-hindbrain level, in the buccal ectoderm at the level of the oral plate and in the foregut endoderm. The red arrowheads point to the boundary of the ANR as defined by *Fgf8* expression domain. (O′) Purple and blue arrowheads delimit the VEAP and the surface ectoderm (SE) laterally. Note that *Six3*, *Hesx1 Foxg1* and *Dlx5* are expressed in the rostral portion of the buccal ectoderm (anterior to the oral plate). (**P**) Linear representation of the gene expression profiles and their overlapping domains at the 7-somite stage. The relative extent of the expression domains (black bars) estimated on histological sections is conserved, except for the surface ectoderm. The *Fgf8* expression domain defines the ANR (hatched red box) encompassing part of the forebrain neuroectodem and the rostral part of the VEAP. (**Q**) The contribution of forebrain and VEAP clones to the ANR. The red dashed line encloses the fitted positions of the HRP-labelled cells scored as contributing to the ANR. Asterisks indicate that one clone originated from two siblings. Scale bars: 110 μm in A for whole-mount images; 60 μm in B for histological sections.

Table 2. Relative contribution of forebrain and VEAP clones to the ANR

Injected zone	Clone no.	Forebrain neuroectoderm	Forebrain cells contributing to ANR	VEAP	VEAP cells contributing to ANR	Total in ANR	Other contribution	Total descendants
INT	11	3	1	3	3	4	BE, SE	10
	12	0	0	5	5	5	–	5
	13*	8	5	6	6	11	MB, HB, BE, SE	35
	18	5	5	3	3	8	–	8
	20	0	0	5	2	2	BE	6
	23	0	0	2	2	2	SE	5
	Subtotal	16	11	24	21	32		69
DIST	26*	30	4	0	0	4	–	30
	27	8	7	2	2	9	MB	17
	29	0	0	3	2	2	–	3
	32	3	1	13	7	8	–	16
	34	4	4	4	4	8	–	8
	39	1	1	3	3	4	–	4
	40	9	4	0	0	4	–	9
	Subtotal	55	21	25	18	39		87

*Clone originated from two siblings.
BE, buccal ectoderm; HB, hindbrain; MB, midbrain; SE, surface ectoderm.

signals cooperate in the specification and positioning of the border cells between neural and non-neural ectoderm (Streit and Stern, 1999; Litsiou et al., 2005; Bailey et al., 2006; Patthey et al., 2009). Cell-labelling studies have established that, at early somite stages, neural plate border cells give rise to sensory placodes at the rostral level and NCCs at caudal levels of the neuraxis (Whitlock and Westerfield, 2000; Bhattacharyya et al., 2004; Jones and Trainor, 2005). Dlx5 is a highly conserved transcription factor which, in the chick embryonic ectoderm, promotes the formation of border cells that subsequently strongly express *Msx1*, *Bmp4* and *Six4* (McLarren et al., 2003). *Dlx5* mouse mutants have late defects in structures derived from border cells, such as the olfactory and otic placodes (Depew et al., 1999; Acampora et al., 1999). Cells in the INT zone could, at an earlier stage (before the formation of the neural plate), be the equivalent of the border cells described in the chick embryo at early somite stages. These mixed fate precursors in the mouse, however, do not express *Dlx5* but do express *Hesx1*. Furthermore, their descendants are not restricted to the prospective placodal region but are widespread throughout the non-neural and neural structures. Alternatively, these progenitors may lie at the prospective boundary between neural and non-neural ectoderm. They might coincide with the region of decay of morphogenetic gradients responsible for the specification of the two neighbouring territories. Often, regions of overlap, where specific precursors intermix, persist at the border of two distinct domains (Woo and Fraser, 1995; Veitia and Salazar-Ciudad, 2007). The intermediate region depicted here is different: it is composed of mixed fate progenitors. The early phase of anterior head formation in the mouse requires considerable growth and complex morphogenesis and therefore a putative pool of mixed fate progenitors could be crucial in providing both neural and non-neural derivatives.

ANR origin and derivatives in mouse and other vertebrates

An important finding is that the non-neural VEAP, which is in direct contact with the anteriormost neuroectoderm but also continuous with buccal and surface ectoderm, has a closer relationship, both spatially and clonally, with the forebrain than with neighbouring, non-neural ectoderm.

The ANR is a well-known signalling centre involved in the specification and regionalisation of the anterior prosencephalon (Houart et al., 2002; Lagutin et al., 2003; Paek et al., 2009). The definition of the ANR varies between vertebrate models, resulting in some inconsistencies in fate maps obtained by grafting or DiI-labelling methods. *Fgf8* expression is often used to define the location of the ANR (Shimamura and Rubenstein, 1997; Vieira et al., 2010), but the onset and extent of *Fgf8* expression vary depending on the species and the developmental stage considered. Here, we define the ANR, on the basis of *Fgf8* expression, as the region encompassing the rostralmost part of the forebrain neuroectodem and the underlying VEAP at the 5- to 7-somite stage. In the chick embryo, the ANR has been described as differentiating from the margin of the neural plate rostral to the anterior limit for NCC formation. A common observation in all studies at early somite stages is that the ANR generates the following ectoderm derivatives: the ventral cephalic epithelium, the olfactory placodes and Rathke's pouch, i.e. the primordium of the anterior pituitary (Couly and Le Douarin, 1985; Couly and Le Douarin, 1987; Eagleson and Harris, 1990; Osumi-Yamashita et al., 1994; Eagleson et al., 1995; Cobos et al., 2001). The *Hesx1*-expressing non-neural ectoderm that contacts the floor of the ventral diencephalon in E8.5 mouse embryos evaginates to form Rathke's pouch at E9.5 (Hermesz et al., 1996; Thomas and Beddington, 1996; Rizzoti and Lovell-Badge, 2005; Gaston-Massuet et al., 2008). Although the HRP-labelled embryos are too young to show any morphological evidence of Rathke's pouch, it is likely, given the results obtained in other animal models, that some precursors of the VEAP are founders of the anterior pituitary primordium. This hypothesis is strongly supported by the genetic fate map of *Hesx1*-expressing cells in the normal mouse embryo (Andoniadou et al., 2007).

Little is known about the origin of the ANR. A study of mid-gastrula stage zebrafish embryos revealed the existence of one row of signalling cells at the margin of the anterior neural plate before the formation of the ANR. These cells, called the anterior neural border (ANB), later contribute to ANR derivatives and telencephalon (Houart et al., 1998). Our data suggest that ANR precursors in the mouse are not confined to the border of the neural plate, as seems to be the case in zebrafish, but are dispersed over a broad area of the anterior ectoderm. The ANR arises both from the intermediate zone composed of mixed fate progenitors and from a more distal region where neural progenitors reside, sometimes sharing common progenitors.

This study, combining cell lineage and gene expression analyses, provides a basis for further investigations into the specification and early regionalisation of the anterior neural plate and for the interpretation of mutant phenotypes.

Acknowledgements
We thank D. Sabéran-Djoneidi, R. Baldock, C. Houart, D. Morello, A. Zwijzen, K. Pakdaman and D. Touati for advice and discussion; H. Morrison for the optical projection tomography work; L. Graham for producing the images for the reconstruction; and A. Perea-Gomez, C. Papanayotou and V. Wilson for critical reading of the manuscript.

Funding
This work was supported by the Centre National de la Recherche Scientifique; the Agence Nationale pour la Recherche [ANR-06-BLANC-0200 to J.C.]; the Association pour la Recherche contre le Cancer [ARC 3715 to J.C.]; the UK Medical Research Council; and the Royal Netherlands Academy of Arts and Sciences (to the Hubrecht Institute to K.A.L.). Deposited in PMC for release after 6 months.

Competing interests statement
The authors declare no competing financial interests.

Author contributions
A.C. conceived and coordinated the project; A.C. and K.A.L. designed experiments; K.A.L. and A.C. performed microinjection experiments and analysed the clones; A.M. processed the HRP-labelled embryos; M.C. and A.C. collected and analysed gene expression data; K.A.L. instigated the 3D reconstruction project, plotted and analysed the clones; A.R. processed the embryo for the 3D reconstruction; J.R. extended the software for the 3D reconstruction; B.H. developed the software for 3D surface and 2D transformation; A.C. planned and wrote the manuscript with contributions of K.A.L., M.C. and J.C.

Supplementary material
Supplementary material available online at
http://dev.biologists.org/lookup/suppl/doi:10.1242/dev.075499/-/DC1

References

Acampora, D., Merlo, G. R., Paleari, L., Zerega, B., Postiglione, M. P., Mantero, S., Bober, E., Barbieri, O., Simeone, A. and Levi, G. (1999). Craniofacial, vestibular and bone defects in mice lacking the Distal-less-related gene Dlx5. *Development* **126**, 3795-3809.
Acampora, D., Postiglione, M. P., Avantaggiato, V., Di Bonito, M. and Simeone, A. (2000). The role of Otx and Otp genes in brain development. *Int. J. Dev. Biol.* **44**, 669-677.
Andoniadou, C. L., Signore, M., Sajedi, E., Gaston-Massuet, C., Kelberman, D., Burns, A. J., Itasaki, N., Dattani, M. and Martinez-Barbera, J. P. (2007). Lack of the murine homeobox gene Hesx1 leads to a posterior transformation of the anterior forebrain. *Development* **134**, 1499-1508.
Ang, S. L. and Rossant, J. (1993). Anterior mesendoderm induces mouse Engrailed genes in explant cultures. *Development* **118**, 139-149.
Ang, S. L., Conlon, R. A., Jin, O. and Rossant, J. (1994). Positive and negative signals from mesoderm regulate the expression of mouse Otx2 in ectoderm explants. *Development* **120**, 2979-2989.
Avilion, A. A., Nicolis, S. K., Pevny, L. H., Perez, L., Vivian, N. and Lovell-Badge, R. (2003). Multipotent cell lineages in early mouse development depend on SOX2 function. *Genes Dev.* **17**, 126-140.
Bailey, A. P., Bhattacharyya, S., Bronner-Fraser, M. and Streit, A. (2006). Lens specification is the ground state of all sensory placodes, from which FGF promotes olfactory identity. *Dev. Cell* **11**, 505-517.
Baldock, R. (2004). A 3D paint program for the Mouse Atlas and gene expression database: Tech Report. http://www.emouseatlas.org/emap/analysis_tools_resources/software/eMAP-apps/MAPaint/paint.pdf.
Beddington, R. S. P. (1981). An autoradiographic analysis of the potency of embryonic ectoderm in the 8th day postimplantation mouse embryo. *J. Embryol. Exp. Morphol.* **64**, 87-104.
Beddington, R. S. (1982). An autoradiographic analysis of tissue potency in different regions of the embryonic ectoderm during gastrulation in the mouse. *J. Embryol. Exp. Morphol.* **69**, 265-285.
Beddington, R. S. P. and Lawson, K. A. (1990). Clonal analysis of cell lineage. In *Postimplantation Mammalian Embryos: a Practical Approach* (ed. A. J. Copp and D. L. Cockcroft), pp. 267-316. Oxford: IRL Press.
Bhattacharyya, S., Bailey, A. P., Bronner-Fraser, M. and Streit, A. (2004). Segregation of lens and olfactory precursors from a common territory: cell sorting and reciprocity of Dlx5 and Pax6 expression. *Dev. Biol.* **271**, 403-414.
Braun, M. M., Etheridge, A., Bernard, A., Robertson, C. P. and Roelink, H. (2003). Wnt signaling is required at distinct stages of development for the induction of the posterior forebrain. *Development* **130**, 5579-5587.
Chan, W. Y. and Tam, P. P. (1986). The histogenetic potential of neural plate cells of early-somite-stage mouse embryos. *J. Embryol. Exp. Morphol.* **96**, 183-193.
Chazaud, C., Oulad-Abdelghani, M., Bouillet, P., Decimo, D., Chambon, P. and Dolle, P. (1996). AP-2.2, a novel gene related to AP-2, is expressed in the forebrain, limbs and face during mouse embryogenesis. *Mech. Dev.* **54**, 83-94.
Cignoni, P., Callieri, M., Corsini, M., Dellepiane, M., Ganovell, F. and Ranzuglia, G. (2008). MeshLab: an open-source mesh processing tool. In *EG It 2008 – Eurographics Italian Chapter Conference (Salerno, 2-4 July 2008)* (ed. V. Scarano, R. De Chiara and U. Erra), pp. 129-136. Geneva, Switzerland: The Eurographics Association.
Cobos, I., Shimamura, K., Rubenstein, J. L., Martinez, S. and Puelles, L. (2001). Fate map of the avian anterior forebrain at the four-somite stage, based on the analysis of quail-chick chimeras. *Dev. Biol.* **239**, 46-67.
Couly, G. F. and Le Douarin, N. M. (1985). Mapping of the early neural primordium in quail-chick chimeras. I. Developmental relationships between placodes, facial ectoderm, and prosencephalon. *Dev. Biol.* **110**, 422-439.
Couly, G. F. and Le Douarin, N. M. (1987). Mapping of the early neural primordium in quail-chick chimeras. II. The prosencephalic neural plate and neural folds: implications for the genesis of cephalic human congenital abnormalities. *Dev. Biol.* **120**, 198-214.
Crossley, P. H., Martinez, S., Ohkubo, Y. and Rubenstein, J. L. (2001). Coordinate expression of Fgf8, Otx2, Bmp4, and Shh in the rostral prosencephalon during development of the telencephalic and optic vesicles. *Neuroscience* **108**, 183-206.
Dattani, M. T., Martinez-Barbera, J. P., Thomas, P. Q., Brickman, J. M., Gupta, R., Martensson, I. L., Toresson, H., Fox, M., Wales, J. K., Hindmarsh, P. C. et al. (1998). Mutations in the homeobox gene HESX1/Hesx1 associated with septo-optic dysplasia in human and mouse. *Nat. Genet.* **19**, 125-133.
Depew, M. J., Liu, J. K., Long, J. E., Presley, R., Meneses, J. J., Pedersen, R. A. and Rubenstein, J. L. (1999). Dlx5 regulates regional development of the branchial arches and sensory capsules. *Development* **126**, 3831-3846.
Downs, K. M. and Davies, T. (1993). Staging of gastrulating mouse embryos by morphological landmarks in the dissecting microscope. *Development* **118**, 1255-1266.
Eagleson, G. W. and Harris, W. A. (1990). Mapping of the presumptive brain regions in the neural plate of Xenopus laevis. *J. Neurobiol.* **21**, 427-440.
Eagleson, G., Ferreiro, B. and Harris, W. A. (1995). Fate of the anterior neural ridge and the morphogenesis of the Xenopus forebrain. *J. Neurobiol.* **28**, 146-158.
Fraser, S., Keynes, R. and Lumsden, A. (1990). Segmentation in the chick embryo hindbrain is defined by cell lineage restrictions. *Nature* **344**, 431-435.
Gardner, R. L. and Cockroft, D. L. (1998). Complete dissipation of coherent clonal growth occurs before gastrulation in mouse epiblast. *Development* **125**, 2397-2402.
Gaston-Massuet, C., Andoniadou, C. L., Signore, M., Sajedi, E., Bird, S., Turner, J. M. and Martinez-Barbera, J. P. (2008). Genetic interaction between the homeobox transcription factors HESX1 and SIX3 is required for normal pituitary development. *Dev. Biol.* **324**, 322-333.
Hatini, V., Ye, X., Balas, G. and Lai, E. (1999). Dynamics of placodal lineage development revealed by targeted transgene expression. *Dev. Dyn.* **215**, 332-343.
Hermesz, E., Mackem, S. and Mahon, K. A. (1996). Rpx: a novel anterior-restricted homeobox gene progressively activated in the prechordal plate, anterior neural plate and Rathke's pouch of the mouse embryo. *Development* **122**, 41-52.
Houart, C., Westerfield, M. and Wilson, S. W. (1998). A small population of anterior cells patterns the forebrain during zebrafish gastrulation. *Nature* **391**, 788-792.
Houart, C., Caneparo, L., Heisenberg, C., Barth, K., Take-Uchi, M. and Wilson, S. (2002). Establishment of the telencephalon during gastrulation by local antagonism of Wnt signaling. *Neuron* **35**, 255-265.
Inoue, T., Nakamura, S. and Osumi, N. (2000). Fate mapping of the mouse prosencephalic neural plate. *Dev. Biol.* **219**, 373-383.
Jones, N. C. and Trainor, P. A. (2005). Role of morphogens in neural crest cell determination. *J. Neurobiol.* **64**, 388-404.
Kobayashi, D., Kobayashi, M., Matsumoto, K., Ogura, T., Nakafuku, M. and Shimamura, K. (2002). Early subdivisions in the neural plate define distinct competence for inductive signals. *Development* **129**, 83-93.
Lagutin, O. V., Zhu, C. C., Kobayashi, D., Topczewski, J., Shimamura, K., Puelles, L., Russell, H. R., McKinnon, P. J., Solnica-Krezel, L. and Oliver, G. (2003). Six3 repression of Wnt signaling in the anterior neuroectoderm is essential for vertebrate forebrain development. *Genes Dev.* **17**, 368-379.
Lawson, K. A., Meneses, J. J. and Pedersen, R. A. (1991). Clonal analysis of epiblast fate during germ layer formation in the mouse embryo. *Development* **113**, 891-911.

Levy, B., Petitjean, S., Ray, N. and Maillot, J. (2002). Least squares conformal maps for automatic texture atlas generation. *ACM Trans. Graph.* **2002**, 362-371.
Litsiou, A., Hanson, S. and Streit, A. (2005). A balance of FGF, BMP and WNT signalling positions the future placode territory in the head. *Development* **132**, 4051-4062.
Martinez-Barbera, J. P., Rodriguez, T. A. and Beddington, R. S. (2000). The homeobox gene Hesx1 is required in the anterior neural ectoderm for normal forebrain formation. *Dev. Biol.* **223**, 422-430.
Martinez-Barbera, J. P., Signore, M., Boyl, P. P., Puelles, E., Acampora, D., Gogoi, R., Schubert, F., Lumsden, A. and Simeone, A. (2001). Regionalisation of anterior neuroectoderm and its competence in responding to forebrain and midbrain inducing activities depend on mutual antagonism between OTX2 and GBX2. *Development* **128**, 4789-4800.
Mathis, L. and Nicolas, J. F. (2002). Cellular patterning of the vertebrate embryo. *Trends Genet.* **18**, 627-635.
Mathis, L. and Nicolas, J. F. (2006). Clonal origin of the mammalian forebrain from widespread oriented mixing of early regionalized neuroepithelium precursors. *Dev. Biol.* **293**, 53-63.
McLarren, K. W., Litsiou, A. and Streit, A. (2003). DLX5 positions the neural crest and preplacode region at the border of the neural plate. *Dev. Biol.* **259**, 34-47.
Meyers, E. N., Lewandoski, M. and Martin, G. R. (1998). An Fgf8 mutant allelic series generated by Cre- and Flp-mediated recombination. *Nat. Genet.* **18**, 136-141.
Nichols, D. H. (1981). Neural crest formation in the head of the mouse embryo as observed using a new histological technique. *J. Embryol. Exp. Morphol.* **64**, 105-120.
Oliver, G., Mailhos, A., Wehr, R., Copeland, N. G., Jenkins, N. A. and Gruss, P. (1995). Six3, a murine homologue of the sine oculis gene, demarcates the most anterior border of the developing neural plate and is expressed during eye development. *Development* **121**, 4045-4055.
Osumi-Yamashita, N., Ninomiya, Y., Doi, H. and Eto, K. (1994). The contribution of both forebrain and midbrain crest cells to the mesenchyme in the frontonasal mass of mouse embryos. *Dev. Biol.* **164**, 409-419.
Paek, H., Gutin, G. and Hebert, J. M. (2009). FGF signaling is strictly required to maintain early telencephalic precursor cell survival. *Development* **136**, 2457-2465.
Patthey, C., Edlund, T. and Gunhaga, L. (2009). Wnt-regulated temporal control of BMP exposure directs the choice between neural plate border and epidermal fate. *Development* **136**, 73-83.
Perea-Gomez, A., Lawson, K. A., Rhinn, M., Zakin, L., Brulet, P., Mazan, S. and Ang, S. L. (2001). Otx2 is required for visceral endoderm movement and for the restriction of posterior signals in the epiblast of the mouse embryo. *Development* **128**, 753-765.
Perea-Gomez, A., Camus, A., Moreau, A., Grieve, K., Moneron, G., Dubois, A., Cibert, C. and Collignon, J. (2004). Initiation of gastrulation in the mouse embryo is preceded by an apparent shift in the orientation of the anterior-posterior axis. *Curr. Biol.* **14**, 197-207.
Petit, A. C. and Nicolas, J. F. (2009). Large-scale clonal analysis reveals unexpected complexity in surface ectoderm morphogenesis. *PLoS ONE* **4**, e4353.
Pevny, L. H., Sockanathan, S., Placzek, M. and Lovell-Badge, R. (1998). A role for SOX1 in neural determination. *Development* **125**, 1967-1978.
Pfister, S., Steiner, K. A. and Tam, P. P. (2007). Gene expression pattern and progression of embryogenesis in the immediate post-implantation period of mouse development. *Gene Expr. Patterns* **7**, 558-573.
Piper, J. and Rutovitz, D. (1985). Data structures for image processing in a C language and Unix environment. *Pattern Recognit. Lett.* **3**, 119-129.
Puelles, L., Fernandez-Garre, P., Sanchez-Arrones, L., Garcia-Calero, E. and Rodriguez-Gallardo, L. (2005). Correlation of a chicken stage 4 neural plate fate map with early gene expression patterns. *Brain Res. Brain Res. Rev.* **49**, 167-178.
Quinlan, G. A., Williams, E. A., Tan, S. S. and Tam, P. P. (1995). Neuroectodermal fate of epiblast cells in the distal region of the mouse egg cylinder: implication for body plan organization during early embryogenesis. *Development* **121**, 87-98.
Rhinn, M., Dierich, A., Le Meur, M. and Ang, S. (1999). Cell autonomous and non-cell autonomous functions of Otx2 in patterning the rostral brain. *Development* **126**, 4295-4304.
Rizzoti, K. and Lovell-Badge, R. (2005). Early development of the pituitary gland: induction and shaping of Rathke's pouch. *Rev. Endocr. Metab. Disord.* **6**, 161-172.
Rubenstein, J. L., Shimamura, K., Martinez, S. and Puelles, L. (1998). Regionalization of the prosencephalic neural plate. *Annu. Rev. Neurosci.* **21**, 445-477.
Schroeder, W., Martin, K. and Lorenson, B. (2007). *The Visualization Toolkit*, 3rd edn. New York: Kitware.
Serbedzija, G. N., Bronner-Fraser, M. and Fraser, S. E. (1992). Vital dye analysis of cranial neural crest cell migration in the mouse embryo. *Development* **116**, 297-307.
Shanmugalingam, S., Houart, C., Picker, A., Reifers, F., Macdonald, R., Barth, A., Griffin, K., Brand, M. and Wilson, S. W. (2000). Ace/Fgf8 is required for forebrain commissure formation and patterning of the telencephalon. *Development* **127**, 2549-2561.
Shimamura, K. and Rubenstein, J. L. (1997). Inductive interactions direct early regionalization of the mouse forebrain. *Development* **124**, 2709-2718.
Simeone, A. and Acampora, D. (2001). The role of Otx2 in organizing the anterior patterning in mouse. *Int. J. Dev. Biol.* **45**, 337-345.
Snow, M. H. (1977). Gastrulation in the mouse: Growth and regionalization of the epiblast. *J. Embryol. Exp. Morphol.* **42**, 293-303.
Streit, A. and Stern, C. D. (1999). Establishment and maintenance of the border of the neural plate in the chick: involvement of FGF and BMP activity. *Mech. Dev.* **82**, 51-66.
Suda, Y., Hossain, Z. M., Kobayashi, C., Hatano, O., Yoshida, M., Matsuo, I. and Aizawa, S. (2001). Emx2 directs the development of diencephalon in cooperation with Otx2. *Development* **128**, 2433-2450.
Tam, P. P. (1989). Regionalisation of the mouse embryonic ectoderm: allocation of prospective ectodermal tissues during gastrulation. *Development* **107**, 55-67.
Thomas, P. and Beddington, R. (1996). Anterior primitive endoderm may be responsible for patterning the anterior neural plate in the mouse embryo. *Curr. Biol.* **6**, 1487-1496.
Tian, E., Kimura, C., Takeda, N., Aizawa, S. and Matsuo, I. (2002). Otx2 is required to respond to signals from anterior neural ridge for forebrain specification. *Dev. Biol.* **242**, 204-223.
Tzouanacou, E., Wegener, A., Wymeersch, F. J., Wilson, V. and Nicolas, J. F. (2009). Redefining the progression of lineage segregations during mammalian embryogenesis by clonal analysis. *Dev. Cell* **17**, 365-376.
Veitia, R. A. and Salazar-Ciudad, I. (2007). Commonalities in fly embryogenesis and mammalian pituitary patterning. *Trends Endocrinol. Metab.* **18**, 261-265.
Vieira, C., Pombero, A., Garcia-Lopez, R., Gimeno, L., Echevarria, D. and Martinez, S. (2010). Molecular mechanisms controlling brain development: an overview of neuroepithelial secondary organizers. *Int. J. Dev. Biol.* **54**, 7-20.
Whitlock, K. E. and Westerfield, M. (2000). The olfactory placodes of the zebrafish form by convergence of cellular fields at the edge of the neural plate. *Development* **127**, 3645-3653.
Wilson, S. W. and Houart, C. (2004). Early steps in the development of the forebrain. *Dev. Cell* **6**, 167-181.
Woo, K. and Fraser, S. E. (1995). Order and coherence in the fate map of the zebrafish nervous system. *Development* **121**, 2595-2609.
Wood, H. B. and Episkopou, V. (1999). Comparative expression of the mouse Sox1, Sox2 and Sox3 genes from pre- gastrulation to early somite stages. *Mech. Dev.* **86**, 197-201.
Xuan, S., Baptista, C. A., Balas, G., Tao, W., Soares, V. C. and Lai, E. (1995). Winged helix transcription factor BF-1 is essential for the development of the cerebral hemispheres. *Neuron* **14**, 1141-1152.
Yang, L., Zhang, H., Hu, G., Wang, H., Abate-Shen, C. and Shen, M. M. (1998). An early phase of embryonic Dlx5 expression defines the rostral boundary of the neural plate. *J. Neurosci.* **18**, 8322-8330.
Yang, Y. P. and Klingensmith, J. (2006). Roles of organizer factors and BMP antagonism in mammalian forebrain establishment. *Dev. Biol.* **296**, 458-475.
Zoltewicz, J. S., Ashique, A. M., Choe, Y., Lee, G., Taylor, S., Phamluong, K., Solloway, M. and Peterson, A. S. (2009). Wnt signaling is regulated by endoplasmic reticulum retention. *PLoS ONE* **4**, e6191.